Coordinating directional switches of multiagent systems with delayed and nonlinear interactions

Shijie Liu,[1] Rui Xiao,[1] Donghua Zhao,[2] and Yongzheng Sun[1,*]
[1]*School of Mathematics, China University of Mining and Technology, Xuzhou 221116, China*
[2]*School of Mathematical Sciences, Fudan University, Shanghai 200433, China*

(Received 7 May 2023; accepted 6 December 2023; published 29 December 2023)

Coordinating directional switches can appear in moving biological groups. Previous studies have demonstrated that the self-driven particle model can effectively describe the directional switching behaviors, but they rarely considered the effect of time delay and nonlinear interactions. Additionally, research on directional switching behavior in multiagent systems is relative few. Therefore we investigate the influence of delayed and nonlinear interactions on the directional switching movement of multiagent systems, in which response delay and transmission delay are considered. Our analysis yields the theoretical mean switching time of the movement direction, revealing that delayed and nonlinear interactions have a significant impact on the directional switches. Specifically, increasing transmission delay can suppress the directional switches when the response delay is greater than or equal to the transmission delay, and increasing transmission delay may promote the directional switching behaviors for large response delay when the response delay is less than the transmission delay. Furthermore, increasing nonlinearity in interactions may first suppress directional switching behaviors and then promote the directional switches. Our results offer valuable insights for developing bioinspired multiagent devices.

DOI: 10.1103/PhysRevResearch.5.043304

I. INTRODUCTION

The coherence of collective motion in many interacting particles or swarming systems is universally present in nature, such as foraging ants [1], swarming locusts [2–4], schooling fish [5,6] or prawns [7], and flocking birds [8–10]. These phenomena have attracted the attention of researchers [11–16]. Many theoretical and empirical studies have emerged to explore the underlying rationale that leads to collective behaviors [1,15,17–19]. Vicsek *et al.* [19] proposed a propelled particle (SPP) model to study the directional switching phenomenon of collective movement groups, where each individual is considered as a particle, and the moving velocity of each particle is determined by the average velocity of the particles in its local neighborhood. Previous studies generally considered the effects of group density, intrinsic noise, master-slave relationship and other factors on directional switches [15,20–22]. Miguel *et al.* considered a variant of the standard Vicsek model [15] in which the interaction is given by an experience-driven scale-free network and discussed the impact of network heterogeneity on the consistency of model states under different group densities. The model can be regarded as a generalization of Vicsek's model [21], where each bird modifies its flight direction according to the weighted average of its neighbor direction, and the entropy maximization equation is used to obtain the values of noise amplitude and the interaction matrix. Ling *et al.* introduced an improved Vicsek model [22] and discussed the effects of group size and noise on particle trajectories and group order.

Many models in previous studies mainly explored the conditions that most of the collective animals are moving at the almost same speed. And a common phenomenon in the biological groups is that collective animals suddenly change their directions. Buhl *et al.* studied the directional switching behaviors of locust larvae and showed that group density is the major factor affecting the change in direction of locust groups [2]. Yates *et al.* obtained that increasing the intensity of noise can promote the ordered directional switches of locust groups [4]. Attanasi *et al.* analyzed the law of information transmission when the flock turned and found that the deviation of some individuals from the average movement direction of the flock is the main reason that caused the directional switches of the flock [23].

As we know, the cooperative control of multiagent systems is widely used in many military and civil fields, such as UAV control [24–26], intelligent transportation [27,28], swarm control [29–31], and so on. The research on multiagent systems focuses on the consensus problem [32–36], the convergence property [37–39], the swarming behavior [40], etc. Gu and Jiang studied the controllability of leader-follower multiagent systems [41], proposing several easy-to-use controllability criteria for multiagent systems. Koh and Sipahi considered the multiagent consensus dynamics with delay to analyze the relation between the self-regulation phenomenon and delayed interaction [42]. If each individual in a group is regarded as an agent, the entire group can be regarded as a multiagent

*yzsung@gmail.com

system. Then directional switching behavior can also exist in multiagent systems such as robot formation. However, the directional switching behaviors of multiagent systems is less mentioned. Accordingly, it is very significant to study the directional switching behaviors of multiagent systems.

Large-scale moving groups will inevitably be affected by time delay [3,43–46]. Sun *et al.* investigated a self-propelled particle model with delayed interactions [3], showing that the mean switching time is an increasing function of time delay. The influence of response and transmission delays on the directional switches of locusts was discussed numerically and analytically [46], wherein the time required for an agent to receive information and adjust its status is the response delay. And the transmission delay is time that the agent receives information, regardless of the time of processing information. The above studies showed that time delay has important effects on directional switching behavior of groups. In addition, previous studies often considered the linear interactions [3,46], ignoring the nonlinearity in interactions [9,47]. Chen *et al.* proposed a piecewise function to depict nonlinear interaction [9] which was found by using the sparse Bayesian learning method and concluded that the strength of nonlinear interactions can affect the average switching frequency of motion direction.

Based on the above, a self-driven particle model with delayed and nonlinear interactions is considered in this paper, in which response delay and transmission delay are considered, respectively. We compute the mean switching time (MST) of mobile agents. The MST is denoted to describe the directional switching behaviors of moving groups, and the larger the MST, the directional switches are less likely to occur. Through numerical and theoretical analysis, we show that MST reduces with the increase of response delay, i.e., increasing response delay can promote the directional switching behavior of multiagent systems. Contrary to the response delay, the increase of transmission delay can increase the mean switching time, i.e., suppress the directional switches of multiagent systems. However, the effects of response and transmission delays will change in the system where both the delays coexist. The MST increases with the increase of group size, first increases and then decreases with the increase of nonlinear interaction, regardless of response delay or transmission delay.

This paper is arranged as follows. In Sec. II we introduce a model with response delay and nonlinear interactions, derive the probability density function and MST, and illustrate the effects of response delay and nonlinear interactions for multiagent systems. In Sec. III we consider the transmission delay in the model, obtain the probability density function and MST, and analyze the influence of transmission delay on MST. In Sec. IV we study the model with both response and transmission delays, and analyze the impact of two time delays on MST. In Sec. V we end this paper with some discussions.

II. MST FOR MULTIAGENT SYSTEMS WITH RESPONSE DELAY

In this part, we consider a multiagent system with N agents. Since each agent only has limited perceptual induction, its motion is only affected by the agents in its local neighborhood. Thus it is supposed that the neighborhood of the ith agent is a circle with the ith agent as the center and a certain distance r as the radius. When the radius of the circle is limited in the interval $\Omega = [0, 1)$, we can represent the neighborhood of the ith agent by $\mathcal{N}_{i,r}(t) = \{j \in \{1, 2, \ldots, N\} | \min(d_{ij}, 1 - d_{ij}) \leqslant r\}$, where $d_{ij} = |X_i - X_j|$. The state and velocity of each agent are denoted by $X_i \equiv X_i(t) \in \Omega$ and $V_i \equiv V_i(t)$ for $i = 1, \ldots, N$, respectively. Considering the case that agents need time to receive and process information, we introduce a Vicsek model with response delay and analyze its impact on MST. Therefore the motion of the multiagent system with response delay and nonlinear interactions can be described by the following system:

$$\begin{aligned} \mathrm{d}X_i &= V_i \mathrm{d}t, \\ \mathrm{d}V_i &= \left[F\left(V_i^{\mathrm{local}}(t-\tau)\right) - V_i(t-\tau)\right]\mathrm{d}t + \eta \mathrm{d}W_i(t), \end{aligned} \tag{1}$$

where $i = 1, \ldots, N$, $\eta > 0$ is the noise strength, $\mathrm{d}W_i$ are the standard white noise (independently sampled for each individual), and $V_i^{\mathrm{local}}(t) = (1/|\mathcal{N}_{i,r}(t)|) \sum_{j \in \mathcal{N}_{i,r}(t)} V_j(t)$ is the average velocity at time t of the agents within the local neighborhood of the ith agent. τ stands for response delay, including the time for the agent to receive information and adjust the state. Then the ith agent in model (1) updates its velocity at time t according to the velocity information of its neighbor agents at time $t - \tau$. The nonlinear interactions are expressed by the following function [9]:

$$F(x) = \begin{cases} w_\alpha x + (1 - w_\alpha)\mathrm{sgn}(x), & |x| > \alpha, \\ 0, & |x| \leqslant \alpha, \end{cases} \tag{2}$$

where $w_\alpha = 1/(1 + \alpha)$, and $\alpha \in [0, 1]$ is an adjustable parameter defining the relative weight in a decision-making manner that agents take the tradeoff between their motion direction and the consistency to their neighbors. It is noted that F vanishes in between $[-\alpha, \alpha]$. In order to explore the influence of response delay and nonlinear interactions on the directional switching behaviors, we ignore the spatial position and only consider the velocity of agent $V_i(t)$. Here we suppose all the agents interact with each other. We define $S(t)$ as the average speed of all agents and have $S(t) \equiv V_i^{\mathrm{local}}(t)$ for arbitrary i. Then we have

$$\mathrm{d}V_i = [F(S(t-\tau)) - V_i(t-\tau)]\mathrm{d}t + \eta \mathrm{d}W_i(t). \tag{3}$$

After taking the average of all equations for $i = 1, \ldots, N$, we can get

$$\mathrm{d}S = [F(S(t-\tau)) - S(t-\tau)]\mathrm{d}t + \frac{\eta}{\sqrt{N}}\mathrm{d}W(t). \tag{4}$$

We first analyze the dynamics of a noise-free time-delay system. We use the Lyapunov exponent to investigate if the delayed multiagent system is undergoing a chaotic behavior [48–52]. And the Lyapunov exponent of the system is calculated by the method proposed by Benettin *et al.* [53]. Figure 1(a) displays the Lyapunov exponent of response delay system without noise, and it can be seen that the Lyapunov exponent is less than 0 for $\tau < 6.9$ and greater than 0 for $\tau \geqslant 6.9$. That is, the response delay system exists in chaos for $\tau \geqslant 6.9$. Figures 1(b) and 1(c) show the time series of the system for $\tau = 6.8$ and $\tau = 7$. The system shows a stable stationary state for $\tau = 6.8$, as shown in Fig. 1(b). However, the system shows chaotic behavior for $\tau = 7$, as shown in

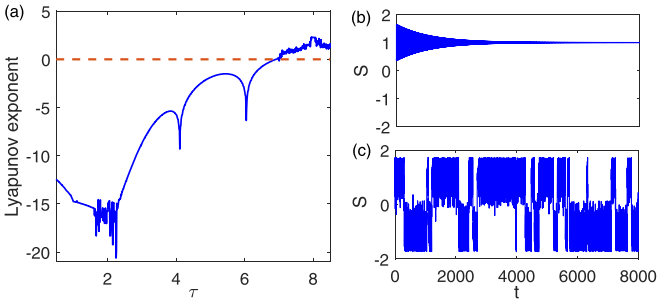

FIG. 1. (a) The Lyapunov exponent of the system (4) without noise as a function of the response delay τ. (b) The time series of the system (4) without noise with $\tau = 6.8$. (c) The time series of the system (4) without noise with $\tau = 7$.

Fig. 1(c). And we can observe the directional switching behavior in Fig. 1(c).

We then analyze the response delay system with noise. To obtain the MST, our analysis is divided into the following three steps. Firstly, the potential function is calculated. Secondly, the analytical expression of P_{st} is obtained. Thirdly, the theoretical result of MST is obtained by parametrizing the time delay.

Assume $P(s,t)$ is the probability density of the stochastic process denoted by Eq. (4). The probability of the global velocity average $S(t) \in [s, s+\mathrm{d}s)$ can be expressed by $P(s,t)\mathrm{d}s$. And the $P(s,t)$ satisfies the following delayed Fokker-Planck equation [54]:

$$\frac{\partial}{\partial t}P(s,t) = -\frac{\partial}{\partial s}\int_{\mathbb{R}}[\mathrm{F}(s_\tau)-s_\tau]P(s,t;s_\tau,t-\tau)\mathrm{d}s_\tau + \frac{\eta^2}{2N}\int_{\mathbb{R}}\frac{\partial^2}{\partial s^2}P(s,t;s_\tau,t-\tau)\mathrm{d}s_\tau, \tag{5}$$

where $s_\tau = s(t-\tau)$, and $P(s,t;s_\tau,t-\tau)$ is the joint probability density of $S(t)$. Let $P_{\mathrm{st}}(s) = \lim_{t\to\infty}P_{\mathrm{st}}(s,t)$ be the stationary probability distribution (SPD) of $S(t)$, and by using the small delay approximation method [54], the first-order approximation of $P_{\mathrm{st}}(s)$ can be obtained as follows:

$$P_{\mathrm{st}}(s) = \frac{AN}{\eta^2}\exp(-\phi(s)), \tag{6}$$

where A is a normalized constant satisfying $\int_{-\infty}^{\infty}P_{\mathrm{st}}(s)\mathrm{d}s = 1$, and $\phi(s)$ is the potential. To get the theoretical expression of P_{st}, we first calculate the potential function $\phi(s)$ defined as $\phi(s) = -2NV_{\mathrm{eff}}(s)/\eta^2$, where the V_{eff} is

$$V_{\mathrm{eff}}(s) = \sqrt{\frac{N}{2\pi\eta^2\tau}}\int_0^s\mathrm{d}s'\int_{-\infty}^{\infty}\mathrm{d}s_\tau[\mathrm{F}(s_\tau)-s_\tau] \times \exp\left(-\frac{[s_\tau - s' - (\mathrm{F}(s')-s')\tau]^2}{2\eta^2\tau/N}\right).$$

Since the F is a piecewise function, we consider the following two cases. Firstly, when $|s| \leqslant \alpha$ we have

$$V_{\mathrm{eff}}(s) = \sqrt{\frac{N}{2\pi\eta^2\tau}}\int_0^s h_{\mathrm{eff}}(s')\mathrm{d}s', \tag{7}$$

with $h_{\mathrm{eff}}(s') = \int_{-\infty}^{\infty}(-s_\tau)\exp(-\frac{[s_\tau - s' - (-s')\tau]^2}{2\eta^2\tau/N})\mathrm{d}s_\tau$. With further calculation we get

$$\begin{aligned} h_{\mathrm{eff}}(s') &= \int_{-\infty}^{\infty}(-s_\tau)\exp\left(-\frac{(s_\tau - s' + s'\tau)^2}{2\eta^2\tau/N}\right)\mathrm{d}s_\tau \\ &= \int_{-\infty}^{\infty}-\mu\exp\left(-\frac{\mu^2}{2\eta^2\tau/N}\right)\mathrm{d}\mu \\ &\quad - \psi(s')\int_{-\infty}^{\infty}\exp\left(-\frac{\mu^2}{2\eta^2\tau/N}\right)\mathrm{d}\mu \\ &= -\psi(s')\int_{-\infty}^{\infty}\exp\left(-\frac{\mu^2}{2\eta^2\tau/N}\right)\mathrm{d}\mu \\ &= -\psi(s')\sqrt{2\eta^2\tau/N}\int_{-\infty}^{\infty}\exp(-\upsilon^2)\mathrm{d}\upsilon \\ &= -\psi(s')\sqrt{2\pi\eta^2\tau/N}, \end{aligned} \tag{8}$$

where $\psi(s') = (1-\tau)s'$, $\mu = s_\tau - \psi(s')$, $\upsilon = \frac{\mu}{\sqrt{2\eta^2\tau/N}}$, and $\int_{-\infty}^{\infty}\exp(-\upsilon^2)\mathrm{d}\upsilon = \sqrt{\pi}$. Therefore we obtain that

$$\begin{aligned} V_{\mathrm{eff}}(s) &= \sqrt{\frac{N}{2\pi\eta^2\tau}}\sqrt{\frac{2\pi\eta^2\tau}{N}}\int_0^s -\psi(s')\mathrm{d}s' \\ &= -\frac{(1-\tau)}{2}s^2 \end{aligned} \tag{9}$$

and

$$\phi(s) = \frac{N}{\eta^2}(1-\tau)s^2. \tag{10}$$

Secondly, we analyze the case of $|s| > \alpha$ and have

$$\begin{aligned} V_{\mathrm{eff}}(s) &= \sqrt{\frac{N}{2\pi\eta^2\tau}}\int_0^\alpha\mathrm{d}s'\int_{-\infty}^{\infty}\mathrm{d}s_\tau(-s_\tau) \\ &\quad\times\exp\left(-\frac{(s_\tau - s' + s'\tau)^2}{2\eta^2\tau/N}\right) \\ &\quad + \sqrt{\frac{N}{2\pi\eta^2\tau}}\int_\alpha^s\mathrm{d}s'\int_{-\infty}^{\infty}\mathrm{d}s_\tau[\mathrm{F}(s_\tau)-s_\tau] \\ &\quad\times\exp\left(-\frac{[s_\tau - s' - (\mathrm{F}(s')-s')\tau]^2}{2\eta^2\tau/N}\right) \\ &\triangleq V_{\mathrm{eff}}^1 + V_{\mathrm{eff}}^2. \end{aligned} \tag{11}$$

For V_{eff}^1, using the previous case analogically, we can get

$$V_{\mathrm{eff}}^1 = -\frac{(1-\tau)}{2}\alpha^2. \tag{12}$$

For V_{eff}^2 we denote

$$V_{\mathrm{eff}}^2(s) = \sqrt{\frac{N}{2\pi\eta^2\tau}}\int_\alpha^s h'_{\mathrm{eff}}\mathrm{d}s', \tag{13}$$

where

$$h'_{\mathrm{eff}}(s') = \int_{-\infty}^{\infty}[\mathrm{F}(s_\tau)-s_\tau] \times\exp\left(-\frac{[s_\tau - s' - (\mathrm{F}(s')-s')\tau]^2}{2\eta^2\tau/N}\right)\mathrm{d}s_\tau. \tag{14}$$

Then we calculate

$$h'_{\text{eff}}(s') = \int_{-\infty}^{\infty} [w_\alpha s_\tau + (1-w_\alpha)\text{sgn}(s_\tau) - s_\tau] \times \exp\left(-\frac{[s_\tau - s' - (w_\alpha s' + (1-w_\alpha)\text{sgn}(s') - s')\tau]^2}{2\eta^2\tau/N}\right) \text{d}s_\tau$$
$$= -\int_{-\infty}^{\infty} (1-w_\alpha) s_\tau \exp\left(-\frac{[s_\tau - \psi(s')]^2}{2\eta^2\tau/N}\right) \text{d}s_\tau + \int_{-\infty}^{\infty} (1-w_\alpha)\text{sgn}(s_\tau) \exp\left(-\frac{[s_\tau - \psi(s')]^2}{2\eta^2\tau/N}\right) \text{d}s_\tau$$
$$\triangleq I_1 + I_2, \tag{15}$$

where $\psi(s') = (1-\tau+w_\alpha\tau)s' + \tau(1-w_\alpha)\text{sgn}(s')$. Using $\mu = s_\tau - \psi(s')$ and $\upsilon = \frac{\mu}{\sqrt{2\eta^2\tau/N}}$, we have

$$I_1 = -\int_{-\infty}^{\infty} (1-w_\alpha) s_\tau \exp\left(-\frac{[s_\tau - \psi(s')]^2}{2\eta^2\tau/N}\right) \text{d}s_\tau$$
$$= -\int_{-\infty}^{\infty} (1-w_\alpha) s_\tau \exp\left(-\frac{\mu^2}{2\eta^2\tau/N}\right) \text{d}s_\tau$$
$$= -(1-w_\alpha)\psi(s') \int_{-\infty}^{\infty} \exp\left(-\frac{\mu^2}{2\eta^2\tau/N}\right) \text{d}s_\tau$$
$$= -(1-w_\alpha)\psi(s')\sqrt{2\pi\eta^2\tau/N}. \tag{16}$$

For I_2 we can simplify that

$$I_2 = (1-w_\alpha) \int_{-\infty}^{\infty} \text{sgn}(s_\tau) \exp\left(-\frac{[s_\tau - \psi(s')]^2}{2\eta^2\tau/N}\right) \text{d}s_\tau$$
$$= -(1-w_\alpha) \int_{-\infty}^{0} \exp\left(-\frac{[s_\tau - \psi(s')]^2}{2\eta^2\tau/N}\right) \text{d}s_\tau + (1-w_\alpha) \int_{0}^{\infty} \exp\left(-\frac{[s_\tau - \psi(s')]^2}{2\eta^2\tau/N}\right) \text{d}s_\tau$$
$$\triangleq I_3 + I_4. \tag{17}$$

Then we obtain

$$I_3 = -(1-w_\alpha) \int_{-\infty}^{-\psi(s')} \exp\left(-\frac{\mu^2}{2\eta^2\tau/N}\right) \text{d}\mu$$
$$= -(1-w_\alpha)\sqrt{2\eta^2\tau/N} \int_{-\infty}^{\frac{-\psi(s')}{\sqrt{2\eta^2\tau/N}}} \exp(-\upsilon^2)\text{d}\upsilon$$
$$= -(1-w_\alpha)\sqrt{2\eta^2\tau/N}\left[\int_{-\infty}^{0} \exp(-\upsilon^2)\text{d}\upsilon + \int_{0}^{\frac{-\psi(s')}{\sqrt{2\eta^2\tau/N}}} \exp(-\upsilon^2)\text{d}\upsilon\right],$$

and

$$I_4 = (1-w_\alpha) \int_{-\psi(s')}^{\infty} \exp\left(-\frac{\mu^2}{2\eta^2\tau/N}\right) \text{d}\mu$$
$$= (1-w_\alpha)\sqrt{2\eta^2\tau/N} \int_{\frac{-\psi(s')}{\sqrt{2\eta^2\tau/N}}}^{\infty} \exp(-\upsilon^2)\text{d}\upsilon$$
$$= (1-w_\alpha)\sqrt{2\eta^2\tau/N}\left[\int_{\frac{-\psi(s')}{\sqrt{2\eta^2\tau/N}}}^{0} \exp(-\upsilon^2)\text{d}\upsilon + \int_{0}^{\infty} \exp(-\upsilon^2)\text{d}\upsilon\right].$$

Thus we have

$$I_3 + I_4 = -(1-w_\alpha)\sqrt{2\eta^2\tau/N}\left[\int_{0}^{\frac{-\psi(s')}{\sqrt{2\eta^2\tau/N}}} \exp(-\upsilon^2)\text{d}\upsilon - \int_{\frac{-\psi(s')}{\sqrt{2\eta^2\tau/N}}}^{0} \exp(-\upsilon^2)\text{d}\upsilon\right]$$
$$= (1-w_\alpha)\sqrt{2\eta^2\tau/N}\left[\int_{0}^{\frac{\psi(s')}{\sqrt{2\eta^2\tau/N}}} \exp(-\omega^2)\text{d}\omega + \int_{\frac{-\psi(s')}{\sqrt{2\eta^2\tau/N}}}^{0} \exp(-\upsilon^2)\text{d}\upsilon\right]$$
$$= (1-w_\alpha)\sqrt{2\eta^2\tau/N} \int_{\frac{-\psi(s')}{\sqrt{2\eta^2\tau/N}}}^{\frac{\psi(s')}{\sqrt{2\eta^2\tau/N}}} \exp(-\upsilon^2)\text{d}\upsilon$$
$$= 2(1-w_\alpha)\sqrt{2\eta^2\tau/N} \int_{0}^{\frac{\psi(s')}{\sqrt{2\eta^2\tau/N}}} \exp(-\upsilon^2)\text{d}\upsilon$$
$$= (1-w_\alpha)\sqrt{2\pi\eta^2\tau/N}\,\text{erf}\left(\frac{\psi(s')}{\sqrt{2\eta^2\tau/N}}\right), \tag{18}$$

where $\omega = -\upsilon$, $\text{erf}(s) = \frac{2}{\sqrt{\pi}} \int_0^s e^{-t^2}\text{d}t$. Therefore we obtain from Eqs. (15)–(18) that

$$h'_{\text{eff}}(s') = (1-w_\alpha)\sqrt{2\pi\eta^2\tau/N}\left[\text{erf}\left(\frac{\psi(s')}{\sqrt{2\eta^2\tau/N}} - \psi(s')\right]\right.$$
$$= (1-w_\alpha)\sqrt{2\pi\eta^2\tau/N}\left[\text{erf}\left(\frac{\psi(s')}{\sqrt{2\eta^2\tau/N}}\right.\right.$$
$$\left.\left. - (1-\tau+w_\alpha\tau)s' - \tau(1-w_\alpha)\text{sgn}(s')\right]\right], \tag{19}$$

and

$$V^2_{\text{eff}}(s) = \sqrt{\frac{N}{2\pi\eta^2\tau}} \int_\alpha^s (1-w_\alpha)\sqrt{2\pi\eta^2\tau/N}\left[\text{erf}\left(\frac{\psi(s')}{\sqrt{2\eta^2\tau/N}}\right)\right.$$
$$\left. - (1-\tau+w_\alpha\tau)s' - \tau(1-w_\alpha)\text{sgn}(s')\right]\text{d}s'.$$

Under conditions $N \gg 1$ and $0 \leqslant \tau < 1$, we can use the asymptotic expansion of the erf function,

$$\int_0^s \text{erf}\left(\frac{\psi(s')}{\sqrt{2\eta^2\tau/N}}\right)\text{d}s' \approx |s|,$$

and

$$V^2_{\text{eff}}(s) \approx -(1-w_\alpha)(1-\tau+w_\alpha\tau)\left(\frac{s^2}{2} - |s|\right) + (1-w_\alpha)(1-\tau+w_\alpha\tau)\left(\frac{\alpha^2}{2} - \alpha\right). \tag{20}$$

According to Eqs. (12) and (20), we can get

$$V_{\text{eff}}(s) = -\frac{(1-\tau)}{2}\alpha^2 - (1-w_\alpha)(1-\tau+w_\alpha\tau)\left(\frac{s^2}{2}-|s|\right) + (1-w_\alpha)(1-\tau+w_\alpha\tau)\left(\frac{\alpha^2}{2}-\alpha\right), \tag{21}$$

and we have

$$\phi(s) = \frac{N}{\eta^2}(1-w_\alpha)(1-\tau+w_\alpha\tau)(s^2-2|s|) - \frac{N}{\eta^2}[w_\alpha(2\tau-1-w_\alpha\tau)\alpha^2 - 2(1-w_\alpha)(1-\tau+w_\alpha\tau)\alpha]. \tag{22}$$

As a result, the stationary probability $P_{\text{st}}(s)$ is summarized as

$$P_{\text{st}}(s) = \begin{cases} \frac{AN}{\eta^2}e^{[-N(1-\tau)s^2/\eta^2]}, & |s| \leqslant \alpha, \\ \frac{A'N}{\eta^2}e^{[-N(1-w_\alpha)(1-\tau+w_\alpha\tau)(s^2-2|s|)/\eta^2]}, & |s| > \alpha, \end{cases} \tag{23}$$

where $A' = LA$, $L = \exp(\frac{N}{\eta^2}[w_\alpha(2\tau-1-w_\alpha\tau)\alpha^2 - 2(1-w_\alpha)(1-\tau+w_\alpha\tau)\alpha])$.

Then, in order to get MST ($T(s)$) of Eq. (4), we calculate the mean first passage time, which represents the mean time cost for a particle jumping from one well of the effective potential to the other. Assume $s=-1$ at $t=0$, and $T(s)$ is the first time that the agents escape from the interval $(-\infty, 0]$. For $|s|>\alpha$ we introduce the nondelay model for obtaining the MST:

$$\mathrm{d}s = [F(s)-s]\mathrm{d}t + \sqrt{2\epsilon_\tau}\mathrm{d}W(t), \tag{24}$$

where $\epsilon_\tau = \eta^2/[2N(1-w_\alpha)(1-\tau+w_\alpha\tau)]$, $0 \leqslant \tau < 1$. It can be seen that Eqs. (4) and (24) have almost the same MST, because they own roughly the same SPD of the effective average velocity. The $T(s)$ satisfies the following equation [55]:

$$(F(s)-s)T'(s) + \epsilon_\tau T''(s) = -1, \tag{25}$$

with the boundary conditions $T(0)=0$ and $\lim T'(s)=0$, and yields

$$T(s) \simeq \frac{2N}{\eta^2}\int_{-1}^{0}\frac{1}{P_{\text{st}}(s)}\mathrm{d}s\int_{-\infty}^{s}P_{\text{st}}(\zeta)\mathrm{d}\zeta. \tag{26}$$

When $s\to 0$, we approximate the probability density function [9] as $P(s) \simeq \frac{AN}{\eta^2}e^{[-N(1-\tau)s^2/\eta^2]}$. And when $s\to -1$, we approximate the probability density function as $P(s) \simeq \frac{A'N}{\eta^2}e^{[-N(1-w_\alpha)(1-\tau+w_\alpha\tau)(s^2+2s)/\eta^2]}$. Thus, we get the following:

$$T \simeq \frac{2N}{\eta^2}\int_{-1}^{0}\frac{1}{P_{\text{st}}(s)}\mathrm{d}s\int_{-\infty}^{0}P_{\text{st}}(\zeta)\mathrm{d}\zeta \simeq \frac{2NA'}{A\eta^2}\int_{-1}^{0}\exp(\frac{N(1-\tau)}{\eta^2}s^2)\mathrm{d}s\int_{-\infty}^{0}\times\exp\left[-\frac{N(1-w_\alpha)(1-\tau+w_\alpha\tau)}{\eta^2}(\zeta^2+2\zeta)\right]\mathrm{d}\zeta. \tag{27}$$

In the process of calculating the above two integrals, we need to use the following two functions:

$$\text{erf}(x) = \frac{2}{\sqrt{\pi}}\int_0^x e^{-t^2}\mathrm{d}t, \quad \text{erfi}(x) = \frac{2}{\sqrt{\pi}}\int_0^x e^{t^2}\mathrm{d}t.$$

For the first integral, we have

$$\int_{-1}^{0}\exp(\frac{N(1-\tau)}{\eta^2}s^2)\mathrm{d}s = \sqrt{\frac{\eta^2}{N(1-\tau)}}\int_{-\sqrt{\frac{N(1-\tau)}{\eta^2}}}^{0}\exp(t^2)\mathrm{d}t = \frac{\eta}{2}\sqrt{\frac{\pi}{N(1-\tau)}}\text{erfi}\left(\sqrt{\frac{N(1-\tau)}{\eta^2}}\right). \tag{28}$$

For the second integral, we obtain

$$\begin{aligned}&\int_{-\infty}^{0}\exp[-\frac{N(1-w_\alpha)(1-\tau+w_\alpha\tau)}{\eta^2}(\zeta^2+2\zeta)]\mathrm{d}\zeta \\ &= \int_{-\infty}^{0}\exp[-p(\zeta^2+2\zeta)]\mathrm{d}\zeta \\ &= e^p\int_{-\infty}^{1}\exp[-p(\zeta+1)^2]\mathrm{d}(\zeta+1) \\ &= \frac{e^p}{\sqrt{p}}\int_{-\infty}^{\sqrt{p}}\exp(-q^2)\mathrm{d}q \\ &= \frac{e^p}{\sqrt{p}}\left[\int_{-\infty}^{0}\exp(-q^2)\mathrm{d}q + \int_0^{\sqrt{p}}\exp(-q^2)\mathrm{d}q\right] \\ &= \frac{e^p}{2}\sqrt{\frac{\pi}{p}}[1+\text{erf}(\sqrt{p})],\end{aligned} \tag{29}$$

where $p = \frac{N(1-w_\alpha)(1-\tau+w_\alpha\tau)}{\eta^2}$, $q = \sqrt{p}(\zeta+1)$. Hence, we get

$$T \simeq \sqrt{\frac{\pi^2}{4(1-w_\alpha)(1-\tau)(1-\tau+w_\alpha\tau)}} \times\left[1+\text{erf}\left(\frac{\sqrt{N(1-w_\alpha)(1-\tau+w_\alpha\tau)}}{\eta}\right)\right] \times\text{erfi}\left(\frac{\sqrt{N(1-\tau)}}{\eta}\right)\exp\left(\frac{N(1-w_\alpha)(1-\tau+w_\alpha\tau)}{\eta^2}\right)L. \tag{30}$$

Through the above analysis, we obtain the theoretical results of the first-order approximation P_{st} and MST, and then theoretically and numerically analyze the effects of group density, response delay, and nonlinear interactions on the directional switching behavior of multiagent systems.

The influence of group size and response delay on directional switches is shown in Fig. 2. Figures 2(a)–2(c) show the numerical results of the average speed S obtained using the standard Euler-Maruyama numerical scheme [56] for different group densities $N=10$, $N=20$, and $N=30$. It can be seen that the average velocity switches from $S<0$ to $S>0$, or from $S>0$ to $S<0$, which can be regarded as a directional switch, representing a phase transition. It can be seen that the directional switching behaviors are more likely to occur in

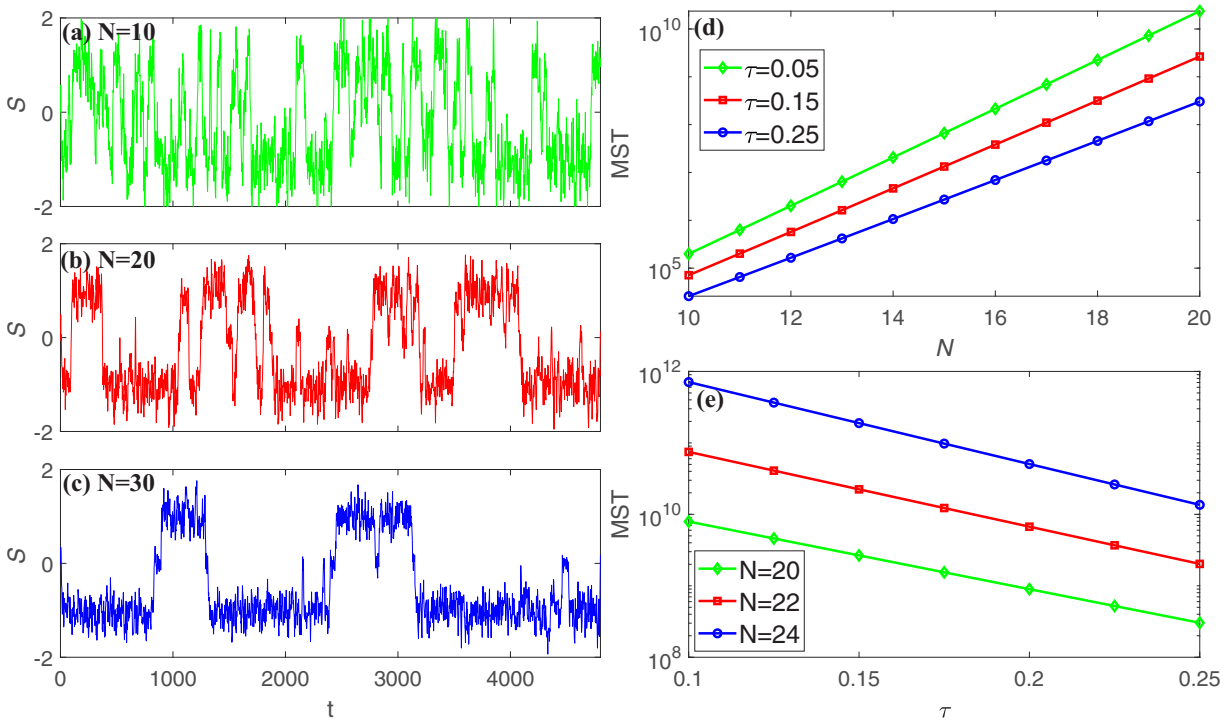

FIG. 2. (a)–(c) The time series of the average speed S obtained from the simulation of system (1) for different group densities $N = 10$, $N = 20$, and $N = 30$, $\tau = 0.1$, and $R = 0.35$. (d) The MST as a function of group size N for three different values of response delay τ. (e) The MST as a function of response delay τ for different values of group size N. The other parameters are set as $\alpha = 0.3$, $\eta = 0.9$. And the results in (d), (e) are the theoretical estimations obtained from Eq. (30).

multiagent system with low group density. Figure 2(d) shows the influence of group density on MST for different response delay. It can be seen that MST is a monotonically increasing function of N. The larger the N, the larger the MST, that is, the agents in multiagent systems are easier to maintain a consistent direction of motion. For any fixed N, it can be read that the larger the response delay, the smaller the MST. That is to say, increasing the response delay can inhibit the direction switching behaviors of multiagent systems. In order to illustrate the effect of response delay on MST more clearly, MST is viewed as a function of response delay for different N in Fig. 2(e). And we see that MST decreases with the increase of response delay. Therefore the larger the response delay, the multiagent system has a higher frequency of direction switches. Comparing Figs. 2(a)–2(c) and Figs. 2(d) and 2(e), it can be seen that the numerical results obtained from Eq. (1) and the theoretical results derived from Eq. (30) have the same conclusion, that is, the larger the group density, the larger the MST.

Then we compare the analytical result derived from Eq. (30) with the result obtained from stochastic simulation based on Eq. (1). Figure 3 illustrates the relationship between the MST and group density N, for $\tau = 0.4$. The numerical results of MST can be obtained by performing long-term stochastic simulations for the original system and counting the number of directional switches. It can be observed that the MST increases as the group density N increases. The theoretical estimation agrees well with the simulation result, particularly for larger values of N, indicating a high consensus between the two approaches.

We further consider the impact of group density on directional switches of multiagent systems from another perspective. Figure 4(a) shows the first-order approximation P_{st} with different values of group density, where the different lines are the theoretical results and the different symbols are the simulation results obtained using the Monte Carlo method. It can be seen that $P_{st}(s)$ has two global maxima at $s = \pm 1$ and a small peak, and the reason why there are peaks in the middle of the figures is that the probability density function is piecewise. When the average velocity is closer to the maxima (the values of $P_{st}(s)$ at $s = \pm 1$), the probability that the system

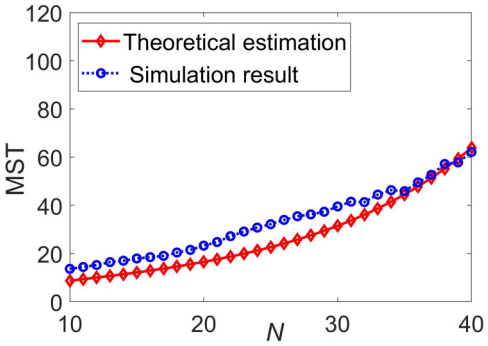

FIG. 3. MST as a function of the group density. The theoretical estimation obtained using Eq. (30) (solid line, diamonds), and the simulation result obtained using simulations of system (1) (dotted line, circles). The parameters are set as $\alpha = 0.68$, $\tau = 0.4$, $\eta = 2$, and $R = 0.35$.

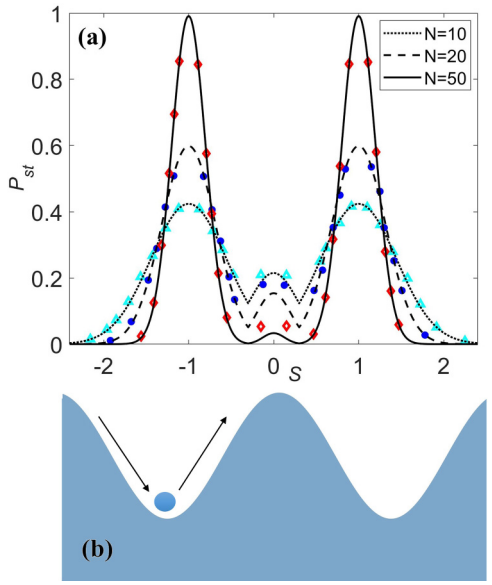

FIG. 4. (a) The P_{st} obtained using Eq. (23) (lines in different types) vs the P_{st} obtained using the stochastic simulations of system (1) (symbols in different types). P_{st} as a function of average velocity S for different group density $N = 10$ (dotted line, triangles), $N = 20$ (dashed line, circles), and $N = 50$ (solid line, diamonds), respectively. The parameters are set as $\tau = 0.5$, $R = 0.5$, $\eta = 0.9$, and $\alpha = 0.3$. (b) A schematic diagram of the potential function.

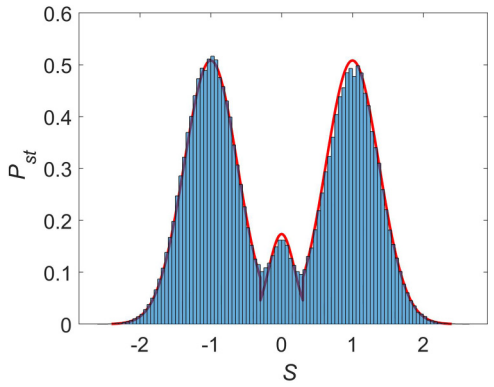

FIG. 6. The stationary distribution of Eq. (23) (solid red line) is compared with the histogram of system (1). The parameter values are $N = 15$, $\eta = 0.9$, $\alpha = 0.25$, $\tau = 0.2$, $R = 0.5$.

keeps the same direction is greater, implying MST is greater. And Fig. 4(a) displays that when $|S| > 0.3$, the larger group density, it is easier for agents in multiagent systems to remain in the same well, i.e., the directional switch frequency of the system is decreased. The results are coincident with Figs. 2 and 3. Moreover, the analysis results match well with the numerical results of the original system. Then Fig. 4(b) shows a schematic diagram of the potential function. The change of parameters can lead to the switch of the ball from one potential well to another, which can be regarded as a phase transition, and the time required for the switch can be defined as the transition time. We use the MST to characterize the frequency of directional switching behavior. The larger the MST, the smaller the frequency of directional switches, i.e., the smaller the frequency of the phase transition.

We explore the effect of nonlinear interactions on MST. Figure 5(a) shows the MST as a function of the nonlinear interactions index α for three different values of response delay. It shows that when $\alpha < 0.15$, the larger the α, the bigger the MST, and when $\alpha > 0.15$, the MST decreases with the increase of α. More specifically, when $\alpha < 0.15$, the stronger the nonlinear interactions, the more difficult it is for individuals in the multiagent system to deviate from the average movement direction of all agents. When $\alpha > 0.15$, the direction switching behaviors of the multiagent system may occur more frequently. Additionally, Fig. 5(b) shows the effect of response delay τ on MST for different α. We see that the larger the τ, the smaller the MST. The result agrees with Fig. 2. And when $\alpha > 0.15$, for fixed τ, the larger the α, the smaller the MST, i.e., increasing the nonlinearity in interactions can increase the number of directional switches. In Fig. 6 we compare the theoretical probability density function Eq. (23) with the time series of the average velocity S from Eq. (1). As seen in Fig. 6, the effect of pairing between the theoretical results and the numerical results of the original system is good, indicating that, above all, the nonlinear interactions

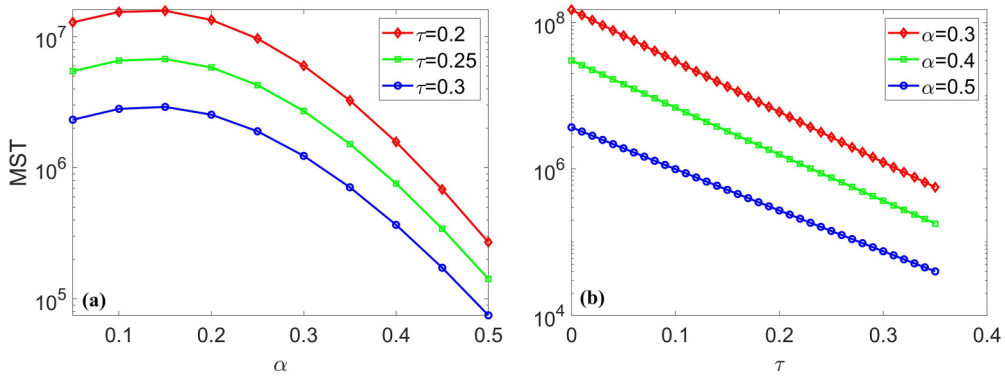

FIG. 5. (a) MST as a function of nonlinearity index α for three different values of response delay τ. (b) MST as a function of response delay τ for different values of nonlinearity index α. The other parameters are set as $\eta = 0.9, N = 15$. The results are the theoretical estimations obtained from Eq. (30).

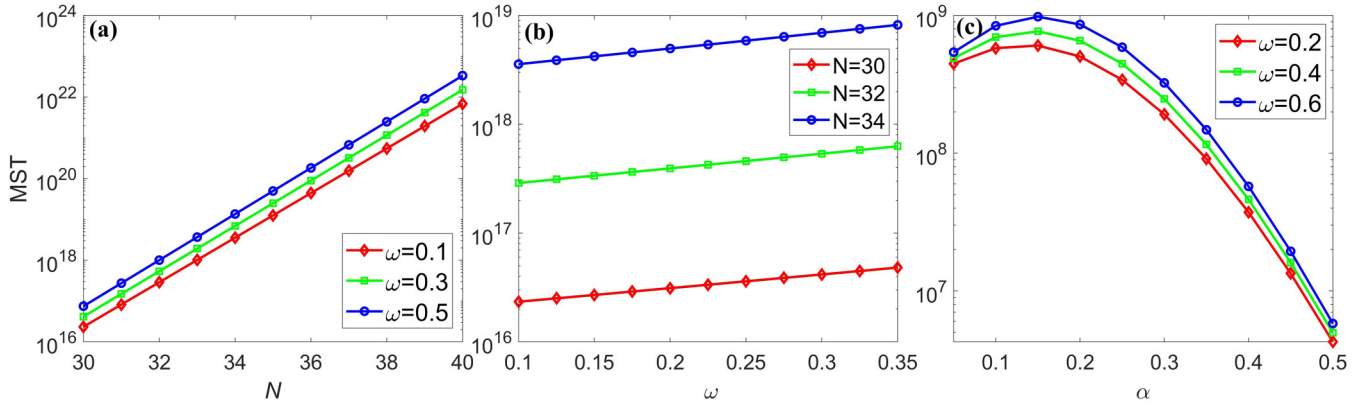

FIG. 7. (a) MST as a function of group size N for three different values of transmission delay ω, $\alpha = 0.3$ and $\eta = 0.9$ are fixed. (b) The MST as a function of transmission delay ω for different group size N, $\alpha = 0.3$ and $\eta = 0.9$ are fixed. (c) MST as a function of nonlinearity index α for three different values of transmission delay ω, $N = 15$ and $\eta = 0.9$ are fixed. The results are the theoretical estimations obtained from Eq. (36).

have an important influence on the directional switches of multiagent systems.

III. MST FOR MULTIAGENT SYSTEMS WITH TRANSMISSION DELAY

The transmission delay also exists in the communication of multiagent systems and represents the time which a moving agent receives the velocity information from its local neighbors. Thus we take the transmission delay into account in the following model:

$$\mathrm{d}V_i = \left[F\left(V_i^{\mathrm{local}}(t-\omega)\right) - V_i(t)\right]\mathrm{d}t + \eta \mathrm{d}W_i(t), \tag{31}$$

in which $F(x)$ is same as the last part, and $\omega > 0$ is the transmission delay. It is noted that the delay does not include the time for the agent to adjust its state. Consequently, the velocity at time t of the ith agent is determined by its own velocity at time t and the mean velocity of its neighbors at time $t-\omega$. Similarly, the average speed $S(t)$ of all the agents satisfies the equation

$$\mathrm{d}S = [F(S(t-\omega)) - S(t)]\mathrm{d}t + \frac{\eta}{\sqrt{N}}\mathrm{d}W(t). \tag{32}$$

Then $P(s,t)$, the probability density function of the global average velocity S, satisfies the following delayed Fokker-Planck equation:

$$\frac{\partial}{\partial t}P(s,t) = -\frac{\partial}{\partial s}\int_{\mathbb{R}}[\mathrm{F}(s_\omega) - s]P(s,t;s_\omega,t-\omega)\mathrm{d}s_\omega + \frac{\eta^2}{2N}\int_{\mathbb{R}}\frac{\partial^2}{\partial s^2}P(s,t;s_\omega,t-\omega)\mathrm{d}s_\omega. \tag{33}$$

We use the small delay approximation method [54] to obtain the first-order approximation of the SPD as

$$P_{\mathrm{st}}^*(s) = \frac{DN}{\eta^2}\exp[-\phi(s)], \tag{34}$$

where D is a normalized constant, and the potential $\phi(s)$ is

$$\phi(s) = \begin{cases} \frac{Ns^2}{\eta^2}, & |s| \leqslant \alpha, \\ \frac{N}{\eta^2}[(1-w_\alpha)(1+w_\alpha w)(s^2-2|s|) + w_\alpha(1-w \\ \quad + w_\alpha w)\alpha^2 + 2(1-w_\alpha)(1+w_\alpha w)\alpha], & |s| > \alpha. \end{cases} \tag{35}$$

And the MST of the multiagent system with transmission delay is approximated as [55]

$$\begin{aligned} T(N,\omega) &\simeq \frac{2N}{\eta^2}\int_{-1}^{0}\frac{1}{P_{\mathrm{st}}^*(s)}\mathrm{d}s\int_{-\infty}^{s}P_{\mathrm{st}}^*(\zeta)\mathrm{d}\zeta \\ &\simeq \frac{2NG'}{\eta^2}\int_{-1}^{0}\exp(\phi(s))\int_{-\infty}^{s}\exp(-\phi(\zeta))\mathrm{d}s\mathrm{d}\zeta \\ &\simeq \sqrt{\frac{\pi^2}{4(1-w_\alpha)(1+w_\alpha\omega)}} \\ &\quad\times\left[1+\mathrm{erf}\left(\frac{\sqrt{N(1-w_\alpha)(1+w_\alpha\omega)}}{\eta}\right)\right] \\ &\quad\times\mathrm{erfi}\left(\frac{\sqrt{N}}{\eta}\right)\exp\left(\frac{N(1-w_\alpha)(1+w_\alpha\omega)}{\eta^2}\right)G', \end{aligned} \tag{36}$$

where $G' = \exp(-N[w_\alpha(1-\omega+w_\alpha\omega)\alpha^2 + 2(1-w_\alpha)(1+w_\alpha\omega)\alpha]/\eta^2)$. Through the above analysis, we can explain the impact of group density, transmission delay, and nonlinear interactions on MST.

Figure 7(a) shows the MST as a function of group density for different values of transmission delay. It can be seen that the MST is a monotonically increasing function of N. Specifically, the larger the group density, the lower the frequency of directional switches of multiagent systems. And for any fixed N, increasing transmission delay can increase MST. Further, Fig. 7(b) displays the MST as a function of transmission delay, and we can get that the larger the transmission delay, the larger the MST, i.e., the directional switching behaviors of the multiagent system is gradually decreased with the increase of transmission delay. To find the impact of nonlinear interactions on MST, we analyze the connection between MST and

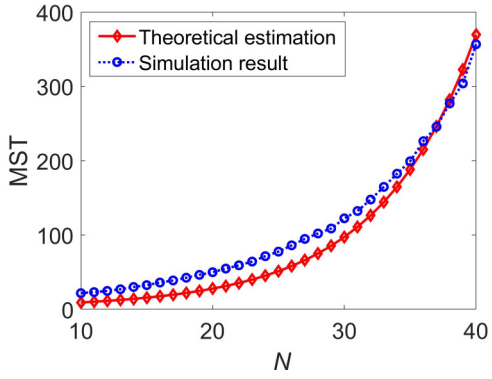

FIG. 8. MST as a function of group density. The theoretical estimation obtained using Eq. (36) (solid line, diamonds), and the simulation result obtained using the simulations of system (31) (dotted line, circles). The parameters are set as $\alpha = 0.668$, $\omega = 0.3$, $\eta = 2$, and $R = 0.35$.

nonlinear interactions in Fig. 7(c). Figure 7(c) plots the MST as a function of the nonlinear interactions index α for different values of transmission delay. It can be observed that the MST increases with the increase of nonlinearity interactions index α in the case of $\alpha < 0.15$ and decreases with the increase of nonlinearity index α in the situation of $\alpha > 0.15$, and these results are consistent with Fig. 5(a).

We compare the analytical result derived from Eq. (36) with the numerical result obtained using Eq. (31). Figure 8 illustrates the relationship between the MST and group density N for $\omega = 0.1$. The numerical results of MST can be obtained by performing long-term stochastic simulations for the original system and counting the number of directional switches. As the group density N increases, the MST is also increases. The simulation result aligns closely with the theoretical estimation, especially for larger values of N.

Next we explain the influence of transmission delay on directional switches of the multiagent system from the aspect of probability density function. Figure 9 plots the first-order approximation P_{st}^* with different values of group density and transmission delay, where the theoretical results obtained from Eq. (34) are drawn as the different lines, and the simulation results of Eq. (31) are plotted as the different symbols. It can be seen that $P_{st}^*(s)$ has two global maxima at $s = \pm 1$, and the probability density function of $|S| < \alpha$ is displayed by the peaks in the middle of Fig. 9. Figure 9(a) shows that when $|S| > 0.3$, the larger the group density, the longer the time for the agents in the multiagent system to maintain a unified direction of motion. As shown in Fig. 9(b), the directional switching behaviors can be more likely to happen in a small ω. Therefore, we conclude that transmission delay has great significance on the directional switching behaviors of the multiagent system. And the theoretical results are in good agreement with the numerical results of the original system.

IV. MULTIAGENT SYSTEMS WITH BOTH RESPONSE AND TRANSMISSION DELAYS

In this section we discuss the influence of response and transmission delays on MST. Then we can take the transmission delay into the system (3), and the model is as follows:

$$dV_i = [F(S(t-\tau)-\omega) - V_i(t-\tau)]dt + \eta dW_i(t), \quad (37)$$

where the parameters are same as the system (3), and $\omega > 0$ is transmission delay. Figure 10 shows the impact of delays on the MST, and we set $\omega = \theta\tau$ with $\theta = 0.5$ ($\tau > \omega$), 1 ($\tau = \omega$), 1.5, and 2 ($\tau < \omega$). Figures 10(a) and 10(b) display the effect of two time delays on the MST for $N = 20$ and $N = 30$, respectively. We can see that for $\tau \geqslant \omega$, with the increase of ω, the MST increases, which means that it can suppress the directional switches. For $\tau < \omega$, the MST shows an increasing trend with the increase of ω for small response delay τ,

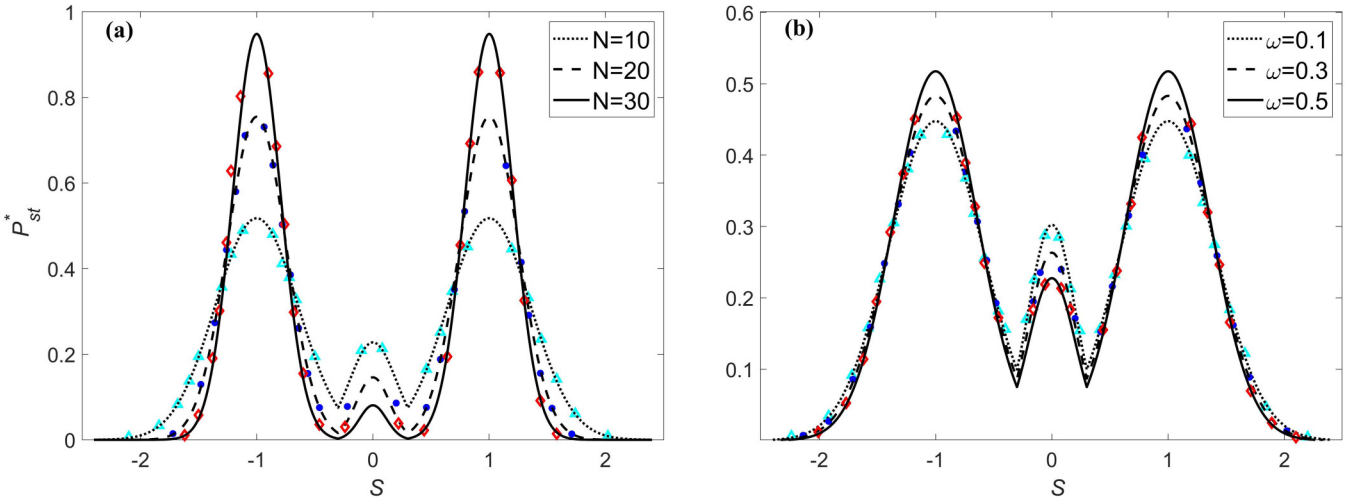

FIG. 9. P_{st}^* obtained using Eq. (34) (lines in different types) vs P_{st}^* obtained using the stochastic simulations of system (31) (symbols in different types). (a) P_{st}^* as a function of average velocity S for different group density $N = 10$ (dotted line, triangles), $N = 20$ (dashed line, circles), and $N = 30$ (solid line, diamonds), respectively, transmission delay $\omega = 0.5$. (b) P_{st}^* as a function of average velocity S for different delays $\omega = 0.1$ (dotted line, triangles), $\omega = 0.3$ (dashed line, circles), and $\omega = 0.5$ (solid line, diamonds), respectively, group size $N = 10$. The other parameters are set as $R = 0.5$, $\alpha = 0.3$, and $\eta = 0.9$.

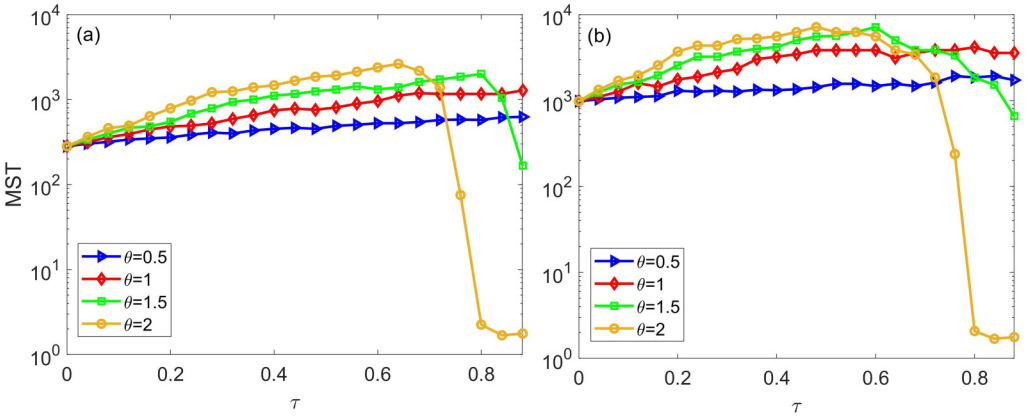

FIG. 10. MST as a function of the response delay τ for system (37) with different values of transmission delay ω, which is expressed by $\omega = \theta\tau$ for $\theta = 0.5, 1, 1.5, 2$: (a) $N = 20$, and (b) $N = 30$. The other parameters are set as $\alpha = 0.3$, $\eta = 0.9$, and $R = 0.5$.

which can inhibit the directional switches, while for a larger response delay τ, the MST decreases with the increase of ω, which can promote the directional switching behaviors. In addition, comparing Figs. 10(a) and 10(b), it can be obtained that the larger the group density, the larger the MST. That is, the increase of group density can reduce the frequency of directional switches.

V. CONCLUSION

In this paper we studied the directional switching behaviors of multiagent systems by a generalized Vicsek model which incorporates both delayed and nonlinear interactions. The first-order approximation of SPD is derived using the small delay approximation method. And the analytical expression of MST of the delayed system is obtained by constructing a nondelayed system which has the same SPD with it. The theoretical and numerical results show that the group density, nonlinear interaction, and time delays can impact on the directional switching behaviors of the system. More precisely, MST increases with the increase of group density, i.e., the frequency of directional switching behavior decreases with the increase of group density. And with the increase of the nonlinear interaction index α, MST first slowly increases and then monotonically decreases, and it can be concluded that the nonlinear interactions are significant for the directional switches of the multiagent system. However, the response and transmission delays have different effects on MST. In the system with response delay only, the frequency of directional switches increases with the increase of delay, while in the system with transmission delay only, the frequency of directional switching behavior decreases with the increase of delay. When the two time delays coexist in the system, we get the conclusion that increasing the transmission can reduce the frequency of directional switching behavior for $\tau \geqslant \omega$. And when the response delay is large enough, increasing the transmission delay can promote the directional switches for $\tau < \omega$. Our work demonstrates the role of nonlinear interactions and delays in directional switching behavior, which has some reference significance for the directional switches of multiagent systems inspired by biology. In addition, in our model all agents in the multiagent system are assumed to be located in a same dimension, without considering the location diversity of agents. In future research we will consider the situation that individuals in multiagent systems are located in different dimensions.

The data and all relevant computer codes that support the findings of this study are available from the corresponding author upon reasonable request.

ACKNOWLEDGMENTS

This work was supported by the National Natural Science Foundation of China (NNSFC) (Grants No. 12271519 and No. 2211001016), the Natural Science Foundation of Jiangsu Province (Grants No. BK20211241 and No. BK20221107), and the Key Research and Development Project of Xuzhou Natural Science Foundation (Grant No. KC23065).

S.L., R.X., D.Z., and Y.S. conceived the project, S.L. and Y.S. analyzed the model, S.L., R.X., D.Z., and Y.S. performed the experiments, all analyzed the data. S.L. wrote the paper with help from R.X., D.Z., and Y.S. R.X, D.Z., and Y.S. contributed equally to this work.

[1] T. Biancalani, L. Dyson, and A. J. McKane, Noise-induced bistable states and their mean switching time in foraging colonies, Phys. Rev. Lett. **112**, 038101 (2014).

[2] J. Buhl, D. J. T. Sumpter, I. D. Couzin, J. J. Hale, E. Despland, E. R. Miller, and S. J. Simpson, From disorder to order in marching locusts, Science **312**, 1402 (2006).

[3] Y. Sun, W. Lin, and R. Erban, Time delay can facilitate coherence in self-driven interacting-particle systems, Phys. Rev. E **90**, 062708 (2014).

[4] C. A. Yates, R. Erban, C. Escudero, I. D. Couzin, J. Buhl, I. G. Kevrekidis, P. K. Maini, and D. J. T. Sumpter, Inherent noise can facilitate coherence in collective swarm motion, Proc. Natl. Acad. Sci. USA **106**, 5464 (2009).

[5] J. Jhawar, R. G. Morris, U. R. Amith-Kumar, M. D. Raj, T. Rogers, H. Rajendran, and V. Guttal, Noise-induced schooling of fish, Nat. Phys. **16**, 488 (2020).

[6] A. Filella, F. Nadal, C. Sire, E. Kanso, and C. Eloy, Model of collective fish behavior with hydrodynamic interactions, Phys. Rev. Lett. **120**, 198101 (2018).

[7] R. P. Mann, A. Perna, D. Strömbom, R. Garnett, J. E. Herbert-Read, D. J. T. Sumpter, and A. J. W. Ward, Multi-scale inference of interaction rules in animal groups using Bayesian model selection, PLoS Comput. Biol. **9**, e1002961 (2013).

[8] D. Chen, B. Xu, T. Zhu, T. Zhou, and H.-T. Zhang, Anisotropic interaction rules in circular motions of pigeon flocks: An empirical study based on sparse Bayesian learning, Phys. Rev. E **96**, 022411 (2017).

[9] D. Chen, Y. Sun, G. Shao, W. Yu, H.-T. Zhang, and W. Lin, Coordinating directional switches in pigeon flocks: The role of nonlinear interactions, R. Soc. Open Sci. **8**, 210649 (2021).

[10] F. Cucker and S. Smale, Emergent behavior in flocks, IEEE Trans. Autom. Control **52**, 852 (2007).

[11] R. Bastien and P. Romanczuk, A model of collective behavior based purely on vision, Sci. Adv. **6**, eaay0792 (2020).

[12] L. Caprini, U. Marini Bettolo Marconi, and A. Puglisi, Spontaneous velocity alignment in motility-induced phase separation, Phys. Rev. Lett. **124**, 078001 (2020).

[13] K. P. O' Keeffe, H. Hong, and S. H. Strogatz, Oscillators that sync and swarm, Nat. Commun. **8**, 1 (2017).

[14] C. Chen, S. Liu, X.-Q. Shi, H. Chaté, and Y. Wu, Weak synchronization and large-scale collective oscillation in dense bacterial suspensions, Nature (London) **542**, 210 (2017).

[15] M. C. Miguel, J. T. Parley, and R. Pastor-Satorras, Effects of heterogeneous social interactions on flocking dynamics, Phys. Rev. Lett. **120**, 068303 (2018).

[16] T. Vicsek and A. Zafeiris, Collective motion, Phys. Rep. **517**, 71 (2012).

[17] C. W. Lynn, L. Papadopoulos, D. D. Lee, and D. S. Bassett, Surges of collective human activity emerge from simple pairwise correlations, Phys. Rev. X **9**, 011022 (2019).

[18] A. Hastings, K. C. Abbott, K. Cuddington, T. Francis, G. Gellner, Y.-C. Lai, A. Morozov, S. Petrovskii, K. Scranton, and M. L. Zeeman, Transient phenomena in ecology, Science **361**, eaat6412 (2018).

[19] T. Vicsek, A. Czirók, E. Ben-Jacob, I. Cohen, and O. Shochet, Novel type of phase transition in a system of self-driven particles, Phys. Rev. Lett. **75**, 1226 (1995).

[20] M. Nagy, Z. Ákos, D. Biro, and T. Vicsek, Hierarchical group dynamics in pigeon flocks, Nature (London) **464**, 890 (2010).

[21] T. Mora, A. M. Walczak, L. Del Castello, F. Ginelli, S. Melillo, L. Parisi, M. Viale, A. Cavagna, and I. Giardina, Local equilibrium in bird flocks, Nat. Phys. **12**, 1153 (2016).

[22] H. Ling, G. E. Mclvor, J. Westley, K. van der Vaart, R. T. Vaughan, A. Thornton, and N. T. Ouellette, Behavioural plasticity and the transition to order in jackdaw flocks, Nat. Commun. **10**, 5174 (2019).

[23] A. Attanasi, A. Cavagna, L. Del Castello, I. Giardina, A. Jelic, S. Melillo, L. Parisi, O. Pohl, E. Shen, and M. Viale, Emergence of collective changes in travel direction of starling flocks from individual birds' fluctuations, J. R. Soc. Interface. **12**, 20150319 (2015).

[24] Huy Xuan Pham, Hung Manh La, D. Feil-Seifer, and M. C. Deans, A distributed control framework of multiple unmanned aerial vehicles for dynamic wildfire tracking, IEEE Trans. Syst. Man Cybern.: Syst. **50**, 1537 (2018).

[25] M. Mozaffari, W. Saad, M. Bennis, and Mérouane Debbah, Efficient deployment of multiple unmanned aerial vehicles for optimal wireless coverage, IEEE Commun. Lett. **20**, 1647 (2016).

[26] S. Huang, Rodney Swee Huat Teo, and Kok Kiong Tan, Collision avoidance of multi unmanned aerial vehicles: A review, Annu. Rev. Control **48**, 147 (2019).

[27] H. Hamidi and A. Kamankesh, An approach to intelligent traffic management system using a multi-agent system, Int. J. Intell. Transp. Syst. Res. **16**, 112 (2018).

[28] Jeancarlo Arguello Calvo and I. Dusparic, Heterogeneous multi-agent deep reinforcement learning for traffic lights control, in *AICS* (CEUR-WS, Dublin, Ireland, 2018), pp. 2–13.

[29] Gökhan M Atınç, Dušan M Stipanović, and P. G. Voulgaris, A swarm-based approach to dynamic coverage control of multi-agent systems, Automatica **112**, 108637 (2020).

[30] A. Cenedese, C. Favaretto, and G. Occioni, Multi-agent swarm control through Kuramoto modeling, in *2016 IEEE 55th Conference on Decision and Control (CDC)* (IEEE, New York, 2016), pp. 1820–1825.

[31] V. Krishnan and S. Martinez, Distributed control for spatial self-organization of multi-agent swarms, SIAM J. Control Optim. **56**, 3642 (2018).

[32] Z. Wang, J. Xu, X. Song, and H. Zhang, Consensus problem in multi-agent systems under delayed information, Neurocomputing **316**, 277 (2018).

[33] Y. Sun, P. Shi, and Cheng-Chew Lim, Event-triggered sliding mode scaled consensus control for multi-agent systems, J. Franklin Inst. **359**, 981 (2022).

[34] H. Dai, Y. Sun, W. Li, and D. Zhao, Multiplicative measurement noise can facilitate consensus of multiagent networks, Phys. Rev. E, **100**, 022319 (2019).

[35] Y. Cao, B. Li, S. Wen, and T. Huang, Consensus tracking of stochastic multi-agent system with actuator faults and switching topologies, Inf. Sci. **607**, 921 (2022).

[36] Y. Dong, J. Chen, and J. Cao, Fixed-time consensus of nonlinear multi-agent systems with stochastically switching topologies, Int. J. Control **95**, 2828 (2022).

[37] L. Li, Y. Yu, X. Li, and L. Xie, Exponential convergence of distributed optimization for heterogeneous linear multi-agent systems over unbalanced digraphs, Automatica **141**, 110259 (2022).

[38] Y. Sun, W. Li, and D. Zhao, Convergence time and speed of multi-agent systems in noisy environments, Chaos **22**, 043126 (2012).

[39] L. Wang and G. Chen, Synchronization of multi-agent systems with metric-topological interactions, Chaos **26**, 094809 (2016).

[40] W. Yu, G. Chen, M. Cao, J. Lü, and Hai-Tao Zhang, Swarming behaviors in multi-agent systems with nonlinear dynamics, Chaos **23**, 043118 (2013).

[41] M. Gu and Guo-Ping Jiang, On the controllability of discrete-time leader-follower multiagent systems with two-time-scale and heterogeneous features, Math. Probl. Eng. **2021**, 13 (2021).

[42] Min Hyong Koh and R. Sipahi, A consensus dynamics with delay-induced instability can self-regulate for stability via agent regrouping, Chaos **26**, 116313 (2016).

[43] R. Erban, J. Haskovec, and Y. Sun, A Cucker–Smale model with noise and delay, SIAM J. Appl. Math. **76**, 1535 (2016).

[44] M. Mijalkov, A. McDaniel, J. Wehr, and G. Volpe, Engineering sensorial delay to control phototaxis and emergent collective behaviors, Phys. Rev. X **6**, 011008 (2016).

[45] R. Olfati-Saber and R. M. Murray, Consensus problems in networks of agents with switching topology and time-delays, IEEE Trans. Automat. Contr. **49**, 1520 (2004).

[46] Y. Sun, W. Li, L. Li, G. Wen, S. Azaele, and W. Lin, Delay-induced directional switches and mean switching time in swarming systems, Phys. Rev. Res. **4**, 033054 (2022).

[47] S. Basu, K. Kumbier, J. B. Brown, and B. Yu, Iterative random forests to discover predictive and stable high-order interactions, Proc. Natl. Acad. Sci. USA **115**, 1943 (2018).

[48] D. V. Senthilkumar and M. Lakshmanan, Transition from anticipatory to lag synchronization via complete synchronization in time-delay systems, Phys. Rev. E **71**, 016211 (2005).

[49] D. V. Senthilkumar, M. Lakshmanan, and J. Kurths, Phase synchronization in time-delay systems, Phys. Rev. E **74**, 035205(R) (2006).

[50] H. Sven, D. Thomas, Y. Serhiy, J. Thomas, F. Valentin, and K. Ido, Strong and weak chaos in nonlinear networks with time-delayed couplings, Phys. Rev. Lett. **107**, 234102 (2011).

[51] L. H. Miranda-Filho, T. A. Sobral, A. J. F. de Souza, Y. Elskens, and Antonio R. de C. Romaguera, Lyapunov exponent in the Vicsek model, Phys. Rev. E **105**, 014213 (2022).

[52] D. Muller-Bender and G. Radons, Laminar chaos in systems with quasiperiodic delay, Phys. Rev. E **107**, 014205 (2023).

[53] G. Benettin, L. Galgani, A. Giorgilli, and J.-M. Strelcyn, Lyapunov characteristic exponents for smooth dynamical systems and for Hamiltonian systems; A method for computing all of them. Part 1: Theory, Meccanica **15**, 9 (1980).

[54] T. D. Frank, Delay Fokker-Planck equations, Novikov's theorem, and Boltzmann distributions as small delay approximations, Phys. Rev. E **72**, 011112 (2005).

[55] C. W. Gardiner *et al.*, *Handbook of Stochastic Methods* (Springer, Berlin, 1985), Vol. 3.

[56] P. E. Kloeden, E. Platen, P. E. Kloeden, and E. Platen, *Stochastic Differential Equations* (Springer, New York, 1992).